SCIENCE CHINA
Life Sciences

SPECIAL TOPIC: Non-resolving inflammation and cancer
• RESEARCH PAPER •

June 2017 Vol.60 No.6: 627–646
doi: 10.1007/s11427-017-9059-y

Decoding early myelopoiesis from dynamics of core endogenous network

Hang Su[1†], Gaowei Wang[1†], Ruoshi Yuan[2], Junqiang Wang[1], Ying Tang[3], Ping Ao[1,2,4,5*] & Xiaomei Zhu[5*]

[1]*Key Laboratory of Systems Biomedicine (Ministry of Education), Shanghai Center for Systems Biomedicine, Shanghai Jiao Tong University, Shanghai 200240, China;*
[2]*School of Biomedical Engineering, Shanghai Jiao Tong University, Shanghai 200240, China;*
[3]*Department of Physics and Astronomy, Shanghai Jiao Tong University, Shanghai 200240, China;*
[4]*State Key Laboratory for Oncogenes and Related Genes, Shanghai Cancer Institute, Shanghai Jiao Tong University School of Medicine, Shanghai 200240, China;*
[5]*Shanghai Center for Quantitative Life Sciences and Physics Department, Shanghai University, Shanghai 200444, China*

Received January 17, 2017; accepted April 27, 2017; published online May 29, 2017

A decade ago mainstream molecular biologists regarded it impossible or biologically ill-motivated to understand the dynamics of complex biological phenomena, such as cancer genesis and progression, from a network perspective. Indeed, there are numerical difficulties even for those who were determined to explore along this direction. Undeterred, seven years ago a group of Chinese scientists started a program aiming to obtain quantitative connections between tumors and network dynamics. Many interesting results have been obtained. In this paper we wish to test such idea from a different angle: the connection between a normal biological process and the network dynamics. We have taken early myelopoiesis as our biological model. A standard roadmap for the cell-fate diversification during hematopoiesis has already been well established experimentally, yet little was known for its underpinning dynamical mechanisms. Compounding this difficulty there were additional experimental challenges, such as the seemingly conflicting hematopoietic roadmaps and the cell-fate inter-conversion events. With early myeloid cell-fate determination in mind, we constructed a core molecular endogenous network from well-documented gene regulation and signal transduction knowledge. Turning the network into a set of dynamical equations, we found computationally several structurally robust states. Those states nicely correspond to known cell phenotypes. We also found the states connecting those stable states. They reveal the developmental routes—how one stable state would most likely turn into another stable state. Such interconnected network among stable states enabled a natural organization of cell-fates into a multi-stable state landscape. Accordingly, both the myeloid cell phenotypes and the standard roadmap were explained mechanistically in a straightforward manner. Furthermore, recent challenging observations were also explained naturally. Moreover, the landscape visually enables a prediction of a pool of additional cell states and developmental routes, including the non-sequential and cross-branch transitions, which are testable by future experiments. In summary, the endogenous network dynamics provide an integrated quantitative framework to understand the heterogeneity and lineage commitment in myeloid progenitors.

†Contributed equally to this work
*Corresponding authors (Ping Ao, email: aoping@sjtu.edu.cn; Xiaomei Zhu, email: xiaomeizhu@yahoo.com)

developmental scheme, early myeloid cell-fate determination, endogenous network, stable state, transition state, landscape

Citation: Su, H., Wang, G., Yuan, R., Wang, J., Tang, Y., Ao, P., and Zhu, X. (2017). Decoding early myelopoiesis from dynamics of core endogenous network . Sci China Life Sci 60, 627–646. doi: 10.1007/s11427-017-9059-y

INTRODUCTION

Long ago it had been pioneered by a few biologists that it should be possible to understand complex phenomena such as cancer from network dynamics perspective. A noticeable example was that of a cancer hallmark paper (Hanahan and Weinberg, 2000). While the hallmarks were regarded sensible, the network had been met with strong resistance and it was regarded as most metaphoric, if not wrong. Indeed, it was soon surely realized that such networks were necessarily incomplete now and in the foreseeable future. Incomplete information problem may be overcome with more and more high-throughput technologies and research efforts, a few additional critical issues were pointed out, nevertheless. For example, even up to current stage of research, most networks in biology are of input-out type, which are logically incomplete. Furthermore, if one would obtain such networks from increasingly higher and higher throughput data, it would not be possible to establish the corresponding dynamical equations because of missing information on kinetic parameters. Those issues have been taken up seriously during the past 18 years. We have been reasoned that it should indeed be possible to understand cancer genesis and progression from network perspective, and hence proposed systematically an endogenous network perspective (Ao et al., 2008). To obtain a minimum understanding, we reasoned that there should be a minimum set of core modules and pathways, for example, (improper) immune response and (abnormal) metabolism, in addition to usual cell cycle and apoptosis. While genome instability and aneuploidy are strongly associated with cancers, we demonstrated that they are not important from mechanistic side, and those phenomena should be explainable by the endogenous network theory (Ao, 2007). The reason is obvious: at least for a time scale much larger than the typical cell cycle time, so-called cancers are still biologically functioning. Even the endogenous network theory had not been yet accepted as a mainstream theory, the revised cancer hallmark paper had taken those ideas (Hanahan and Weinberg, 2011). The important hallmarks adding into the revised are: deregulating cellular energetics; avoiding immune destruction; genome instability and mutation; tumor-promoting inflammation, four of them discussed during the process to establish the endogenous network theory. On the quantitative side, for nearly 10 years network dynamical modeling for various specific cancers has also demonstrated the essential correctness of endogenous network approach (Wang et al., 2016; Yuan et al., 2016). A question naturally arises: if it is a general biological theory, it should be applicable to normal biological processes, too. In the present article we apply the theory to an experimentally well-established process: a specific hematopoiesis, early developmental stages of myeloid cells.

Blood contains various cell types generated daily in the bone marrow with rapid turnover rates. The tightly regulated hematopoietic development plays key roles in establishment and maintenance of blood homeostasis (Orkin and Zon, 2008). Revealing the cell-fate determination and coordination during hematopoiesis is of great significance and contributes to elucidating the genesis of malignant or aplastic diseases (Tenen, 2003; Young et al., 2008). A standard roadmap of hematopoietic development has been established from a wide range of experimental observations (Figure S1 in Supporting Information): hematopoietic stem cells (HSCs), characterized by their durably self-renewal capacity, lie on the top of the stream; downstream of HSCs are pools of cell intermediates (also known as progenitors) that successively undergo a step-by-step fate restriction (Akashi et al., 2000; Kondo et al., 1997; Weissman, 2000). Specifically, HSCs give rise to multi-potent progenitors (MPPs) that generate two major lineage-restricted intermediates: common lymphoid progenitors (CLPs) and common myeloid progenitors (CMPs). CLPs lose myeloid potential, but retain the ability to form all lymphoid lineage cells. CMPs subsequently develop into more specific progenitors, including megakaryocyte/erythrocyte progenitors (MEPs) and granulocyte/monocyte progenitors (GMPs). These bi-potent progenitors further develop into distinct myeloid cell types: erythrocytes and megakaryocytes from MEPs, granulocytes and monocytes from GMPs. The standard roadmap, which highlights the stepwise and hierarchical manner of hematopoietic development, serves as an operational paradigm for understanding the multi-lineage diversification from a stem cell pool (Bryder et al., 2006).

Although such a hematopoietic scheme was well established experimentally, little has been known about its underpinning organization principles. In addition, many aspects of the hematopoietic development are still controversial. For example, further experimental evidences have led to a series of revisions of the standard roadmap, but a clear consensus on hematopoiesis is still missing (Adolfsson et al., 2005; Yamamoto et al., 2013); the “reprogramming” or “trans-pro-

gramming" events have been extensively observed in experiments, which raised questions for the hierarchical model of development (Graf, 2011; Ji et al., 2013; Riddell et al., 2014). In this work, we sought a comprehensive and quantitative understanding of cell-fate organization during hematopoietic development.

Network models, based on the assumption that genotypes are in general related to phenotypes by a network of biochemical reactions, have shown considerable promise in recent years for revealing the underlying molecular basis of biological phenomenon (Ao et al., 2008; Cahan et al., 2014). Two main and opposite approaches have been used: one is to use various bioinformatics and statistical tools to infer the networks from data; the other is to seek for the causal relations among molecular agents. Along the latter approach, we have introduced an endogenous molecular-cellular network theory based on salient properties of biological system (Ao et al., 2008; Wang et al., 2013; Zhu et al., 2004). Taking early myeloid cell-fate determination as an illustrative example, we constructed a core endogenous network by integrating the accumulated gene regulation and signal transduction knowledge. We quantified the core network and obtained a set of structurally robust states, including 13 stable states and 42 unstable states. Comparing with independent experimental observations and data, we found that the stable states captured the core features of certain cell-fates in early myeloid development, such as the quiescent or apoptotic erythrocytes, and that the unstable states captured the core features of cell intermediates, such as GMPs and MEPs. The transition between stable states is more probable passing through certain unstable state, and further analysis revealed that the interconnections among these robust states accorded with the known developmental routes, which enabled a natural organization of different cell-fates into a multi-stable state "landscape" (Takahashi and Yamanaka, 2015; Waddington, 1942; Wright, 1932).

Accordingly, we obtained a quantitative developmental scheme to understand the early myeloid cell-fate determination, which led to several attractive consequences. Firstly, the quantitative model mechanistically explained the myeloid phenotypes and standard roadmap model in a straightforward way. The stepwise fate-restriction can be envisaged as the process that a cell transits from stem cell state to specialized cell state, successively passing through a series of unstable states representing certain cell intermediates. Secondly, some seemingly controversial observations are expected from the landscape point of view and can be integrated into a single model in principle. The endogenous network dynamics explained and integrated several revised roadmap models and the cell-fate inter-conversion events coherently, including myeloid-bypass model (Yamamoto et al., 2013), megakaryocyte-biased model (the counterpart of LMPP model) (Sanjuan-Pla et al., 2013) and the myeloid trans-differentiation events under specific gene manipulation (Graf, 2002). Thirdly, the endogenous network dynamics predicted the existence of additional cell intermediates and developmental routes, including the non-sequential and cross-branch transitions, testable by future experiments. In summary, the present quantitative model provides a comprehensive understanding towards the hard-wiring of myeloid cell-fates and suggests a more complex picture of development than previous thought.

RESULTS

Core endogenous network of early myeloid cell-fate determination

Hematopoiesis is a highly orchestrated developmental process, where the cell fate options, including self-renewal, cell death, metabolism and lineage-specification, are tightly regulated to maintain the homeostasis of blood system (Folmes et al., 2012; Orkin and Zon, 2008; Weissman, 2000; Zhao and Li, 2015). Taking early myeloid cell-fate determination as an example, we constructed a core endogenous network by integrating the well-documented knowledge to reveal the underlying molecular basis. Endogenous network was defined as a molecular-cellular network shaped by million years of evolution, whose core structure and main properties are conserved (Ao et al., 2008; Wang et al., 2013; Yuan et al., 2017). A set of essential modules, including cell cycle, metabolism, apoptosis and differentiation, was selected to capture the core features of early myeloid development. According to the well-documented gene regulation and signal transduction knowledge (Alberts et al., 2008), each module was simplified and specified by a set of key agents to capture the main functional status (Tables S1 and S2 in Supporting Information). The interactions among agents were summarized from well-documented gene regulation and signaling transduction with solid bio-chemical basis (Table S3 in Supporting Information). Given the universal existence and significance of feedback regulations in biological system (Thomas et al., 1995), the network was organized closed. Accordingly, a core endogenous network of early myeloid cell-fate determination was constructed, which included 45 agents and 177 interactions (Figure 1). It should be admitted that many details have been simplified in the core endogenous network. Indeed, functional modules involved in early myeloid development are far more than the four modules selected above; large amounts of agents have not been included in the present model yet. However, we will show in the following parts that, despite such simplification, the dynamics of this core network have already been able to capture the core features of early myeloid development, and to provide a series of clear-cut predictions.

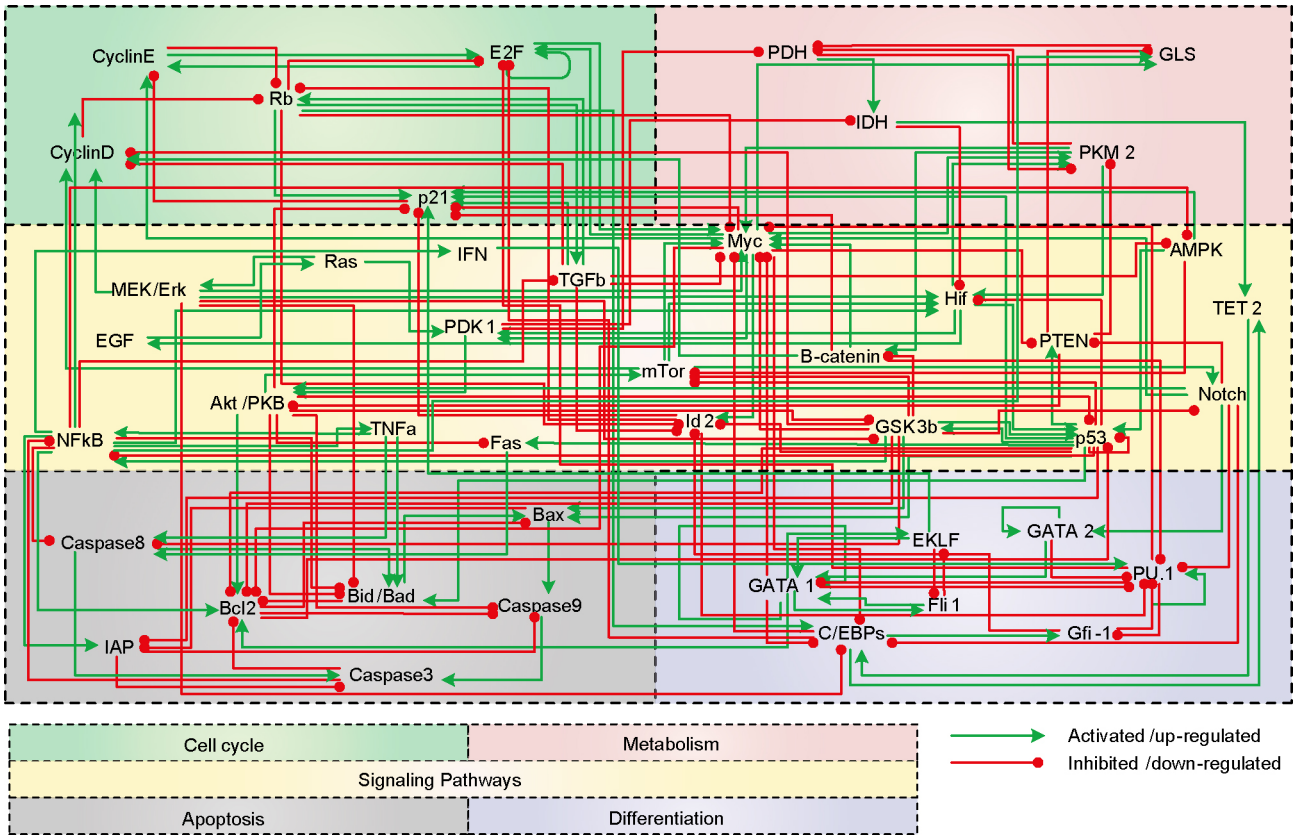

Figure 1 Core endogenous network for early myeloid development. The core endogenous network was formed by a minimal set of essential modules, including cell cycle, metabolism, apoptosis and differentiation. Each module was specified by a set of key agents, which interconnected with each other via signaling pathways and gene regulations. The green line denotes the activated/up-regulated interactions, while the red line denotes the inhibited/down-regulated interactions among these agents, and the arrow or dot represents the direction of interaction.

Quantitative analysis provided unparalleled precision to reveal the emerging properties of complex systems that were difficult to be understood by intuition or linear reasoning alone (Qian, 2013). Therefore, the core endogenous network was further described quantitatively by a non-linear dynamical system. The fixed points, in which system would remain stationary unless perturbation occurred, were calculated and analyzed. Mathematically, fixed points were classified into two types: stable states, characterized by all negative eigenvalues in the real part of the Jacobian matrix, and unstable states, characterized by at least one positive eigenvalue in the real part of the Jacobian matrix (Arnold and Levi, 1988). In a stable state, the system is insensitive to small perturbations and tends to return to the initial stable state when small perturbation occurs; while in an unstable state, the system is more sensitive and would evolve to certain stable states upon perturbation. From the landscape point of view, the stable states can be envisaged intuitively as basins and the unstable states can be viewed as peeks or saddles between neighboring basins (Figure 2A and B). The transition between stable states is more probable passing through certain unstable states. Therefore, the unstable states with single positive eigenvalue in the real part of their Jacobian matrix, commonly known as saddles, were defined as transition states (of rank 1). The unstable states with n ($n \geqslant 2$) positive eigenvalues in the real part of their Jacobian matrix were defined as hyper-transition states of rank n.

Specifically, the core endogenous network was described by a set of ordinary differential equations (ODEs). Since many detailed mechanisms and parameters of the agent interactions are still unknown, we considered a trade-off between model tractability and details, and used a dimensionless modeling framework here by normalizing the agent values that range continuously between 0 and 1. "0" represented complete inactivation, while "1" represented full activation. Here, we mainly focus on fixed points, whereas some more complex features of the dynamical system, such as the limit cycles, will not be discussed in detail at the first stage. We obtained a striking result that 13 stable states (Tables S5−S16, S34 in Supporting Information) and 42 unstable states (Tables S17−S20, S35−S38 in Supporting Information) robustly existed by using different equation forms or parameter values (Table S4 in Supporting Information), when setting 0.5 as threshold to classify each agent as activated or inactivated (represented as 1/0). The threshold can be selected within a range from 0.3 to 0.7, which will not affect the main conclusions. To check the internal consistency of modeling, the core endogenous network was further approximated by

the Boolean dynamics (Supplementary 2.2 in Supporting Information). Thirteen stable states were obtained (Table S21 in Supporting Information), which perfectly agreed with the stable states obtained in ODE dynamical system. We had showed elsewhere that fixed points found by ODEs will correspond to those in stochastic differentiation equations (SDEs), by using a new stochastic integration (Tang et al., 2014a, b; Tang et al., 2014c; Yuan and Ao, 2012). The results demonstrated that these states were determined by the topology of the endogenous network rather than by the selected equation forms or parameter values. The statistical significance of multi-stability of endogenous network dynamics was tested (Figure 2C).

Robust stable states reproduced the core features of certain cell-fates

The concept of stable state has been widely used to represent stable cell phenotypes (Ao et al., 2008; Huang et al., 2009; Wang et al., 2013). The biological meanings of each stable state generated from the core endogenous network have been analyzed at the modular level. The status of cell cycle, apoptosis, metabolism and differentiation was specified by the agent values in each state (Models and methods, Supplementary 3.1 in Supporting Information). In specific, the status of cell cycle and apoptosis was described by 'On' or 'Off', while the metabolism status was described as 'Aerobic' or 'Anaerobic'. The status of differentiation module was specified by a set of activated/highly-expressed lineage-specific TFs. Since the expression of lineage-specific TFs in differentiation module served as the molecular identity of each cell type (Laiosa et al., 2006; Rosenbauer and Tenen, 2007), the 13 stable states were classified into six groups (G1-G6) based on their differentiation module status (Table 1).

In the standard roadmap (Akashi et al., 2000), five stable cell types, including HSCs, neutrophils (granulocytes), monocytes, erythrocytes and megakaryocytes, existed in the early myeloid development (Figure S1 in Supporting Information). Functional status of the five cell types was summarized from well-documented experimental observations (Table 2A). In specific, HSCs were characterized by

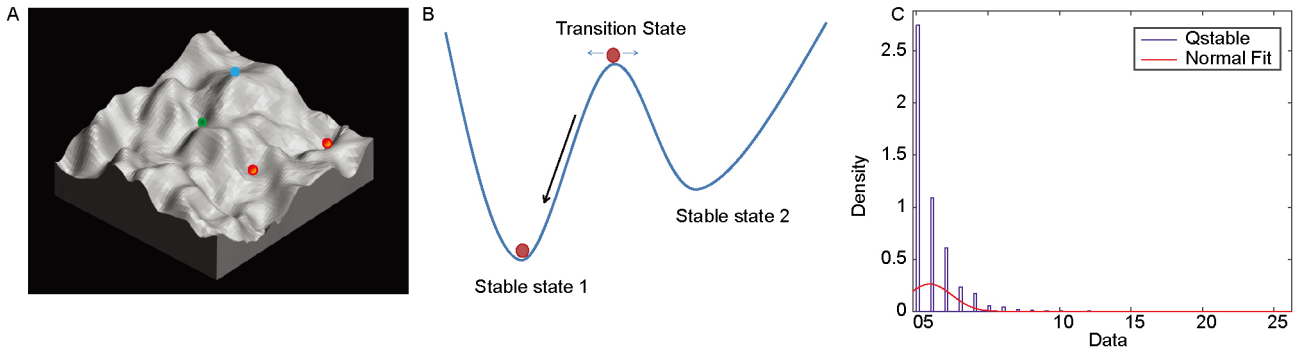

Figure 2 Quantifying the endogenous network. A, The fixed points (stable states and unstable states). Stable states can be envisaged as wells with low potential energy, in which the system will be insensitive to small perturbations (red node). Unstable states can be viewed as peeks or saddles between neighboring wells. The unstable states with one positive eigenvalue (known as saddles) were defined as transition states (green node), while the unstable states with n positive eigenvalues were defined as hyper-transition states of n rank (blue node). B, Interconnection among states. Upon perturbations, the system in an unstable state will evolve to specific stable states. C, The statistical significance of multi-stability of endogenous network dynamics. To assess the statistical significance of the multi-stable states generated from the core endogenous network versus what would be expected by chance, we quantified 10,612 randomized networks by using Boolean analysis and computed the number of stable states Qstable in each randomized network. The distribution of the number of stable states (Qstable) generated by each randomized network is shown in this figure.

Table 1 The module status of the robust stable states and the classification[a)]

Stable state	Group 1			Group 2		Group 3		Group 4		Group 5		Group 6	
	N1	N2	N3	N4	N5	N6	N7	N8	N9	N10	N11	N12	N13
Cell cycle	On	On	Off	Off	Off	Off	Off	Off	Off	Off	Off	Off	Off
Apoptosis	Off	Off	Off	Off	On	On	On	On	On	Off	On	Off	On
Metabolism	Anaer-obic	Anaer-obic	Anaer-obic	Aero-bic	Aero-bic	Aero-bic	Aero-bic	Aero-bic	Aero-bic	Aerobic	Aero-bic	Aerobic	Aero-bic
Differentiation	GATA-2			C.EBPs Gfi-1		PU.1 C/EBPs Egr/Nab		GATA-1 EKLF		GATA-1 Fli-1		GATA-2 C/EBPs Gfi-1	

a) The module status of cell cycle, apoptosis, metabolism and differentiation was specified by the specific agent values in each module. As lineage-specific TFs in the differentiation module served as a molecular identity of each cell type, the 13 stable states were divided into six groups according to their differentiation module status.

their durably self-renewal capacity, resistance of cell death and anaerobic metabolism for energy supplement (Kohli and Passegué, 2014; Weissman, 2000). The emergence and maintenance of HSCs required the activation of a series of specific TFs, illustrated by GATA2 (Grass et al., 2006). In this context, the module status of HSCs was described as cell cycle "on", apoptosis "off", anaerobic metabolism and the highly expressed GATA2 without other lineage-specific TFs expressed in its differentiation module. Similarly, the four specialized cell types at early committed stage, including neutrophils, monocytes, erythrocytes and megakaryocyte, were characterized at modular level (Table 2A).

When comparing the model results with the experimental observations at the modular level, we found that the differentiation module status of the five groups of stable states (G1−G5) captured the molecular identities of HSCs, neutrophils, monocytes, erythrocytes and megakaryocytes respectively (Tables 1 and 2A, Supplementary 3.2 in Supporting Information). We further dissected the stable states in each group according to their module status of cell cycle, apoptosis and metabolism. The results showed that stable states N2, N4, N6, N8, and N10 had good agreements with the functional status of HSCs, neutrophils, monocytes, erythrocytes and megakaryocytes respectively. Stable state N1 described the proliferating stem-like cells with immune responses (details in Supplementary 3.2 in Supporting Information), which were usually observed in some physiological process such as inflammation or carcinogenesis (Coussens and Werb, 2002). Stable state N3 described the quiescent stem cells. Stable state N5, N7, N9, and N11 described the apoptotic states of neutrophils, monocytes, erythrocytes, and megakaryocytes respectively. Besides, we found two robust stable states with highly expressed GATA-2, C/EBPs, Gfi-1 in group 6, which may represent other myeloid cell fates (Iwasaki et al., 2006).

Furthermore, we validated the preliminary conclusions at the molecular level. Firstly, we compared the agent values of stable states N2, N4, N6, N8, and N10, which described the functional status of HSCs, neutrophils, monocytes erythrocytes and megakaryocytes respectively, with the human gene expression data of these five cell types in a published dataset (Novershtern et al., 2011). The agreements between model results and the experimental data were more than 60% (Figure 3A, Models and methods). Considering the conservation of the core endogenous network, we further compared the model results with a hematopoietic expression dataset collected from mice (Chambers et al., 2007), which also showed good agreements (Figure 3B). It should be emphasized that the robust states were obtained by computing the core endogenous network that was constructed from independent gene regulation and signal transduction knowledge. These emerging patterns of robust states were an unanticipated consequence of the endogenous network dynamics, rather than an input to it. Given the limited accuracy of experimental measurements and the simplification in our network construction, the results suggested good agreements between model results and expression data.

Briefly, five robust stable states (N2, N4, N6, N8, N10) of the endogenous network corresponded to the functional status of HSCs, neutrophils, monocytes, erythrocytes, megakaryocytes at both modular and molecular level. The results indicated that the robust stable states of the core endogenous net-

Table 2 Validation of core endogenous network at the modular level[a)]

A. Experimental knowledge					
Cell types	HSC	Neutrophils	Monocytes	Erythrocytes	Megakaryocytes
Cell cycle	On	Off	Off	Off	Off
Apoptosis	Off	Off	Off	Off	Off
Metabolism	Anaerobic	Aerobic	Aerobic	Aerobic	Aerobic
Differentiation	GATA2	C/EBPα PU.1 Gfi-1	PU.1 C/EBPα Egr/Nab	GATA1 EKLF	GATA1 Fli-1
B. Model results					
Stable state	N2	N4	N6	N8	N10
Cell cycle	On	Off	Off	Off	Off
Apoptosis	Off	Off	Off	Off	Off
Metabolism	Anaerobic	Aerobic	Aerobic	Aerobic	Aerobic
Differentiation	GATA2	C/EBPs Gfi-1	PU.1 C/EBPs Egr/Nab	GATA1 EKLF	GATA1 Fli-1

a) A, The functional status of HSCs and four specialized cell types at early committed stage, including neutrophils, monocytes, erythrocytes and megakaryocytes, was summarized from the well-documented observations in the literature (Kohli and Passegue, 2014; Kondo et al., 2003; Rosenbauer and Tenen, 2007). B, The module status of stable states N2, N4, N6, N8, and N10 was obtained from the model. The results showed that stable states N2, N4, N6, N8, and N10 have good matches with the functional status of HSCs, neutrophils, monocytes, erythrocytes and megakaryocytes at the modular level.

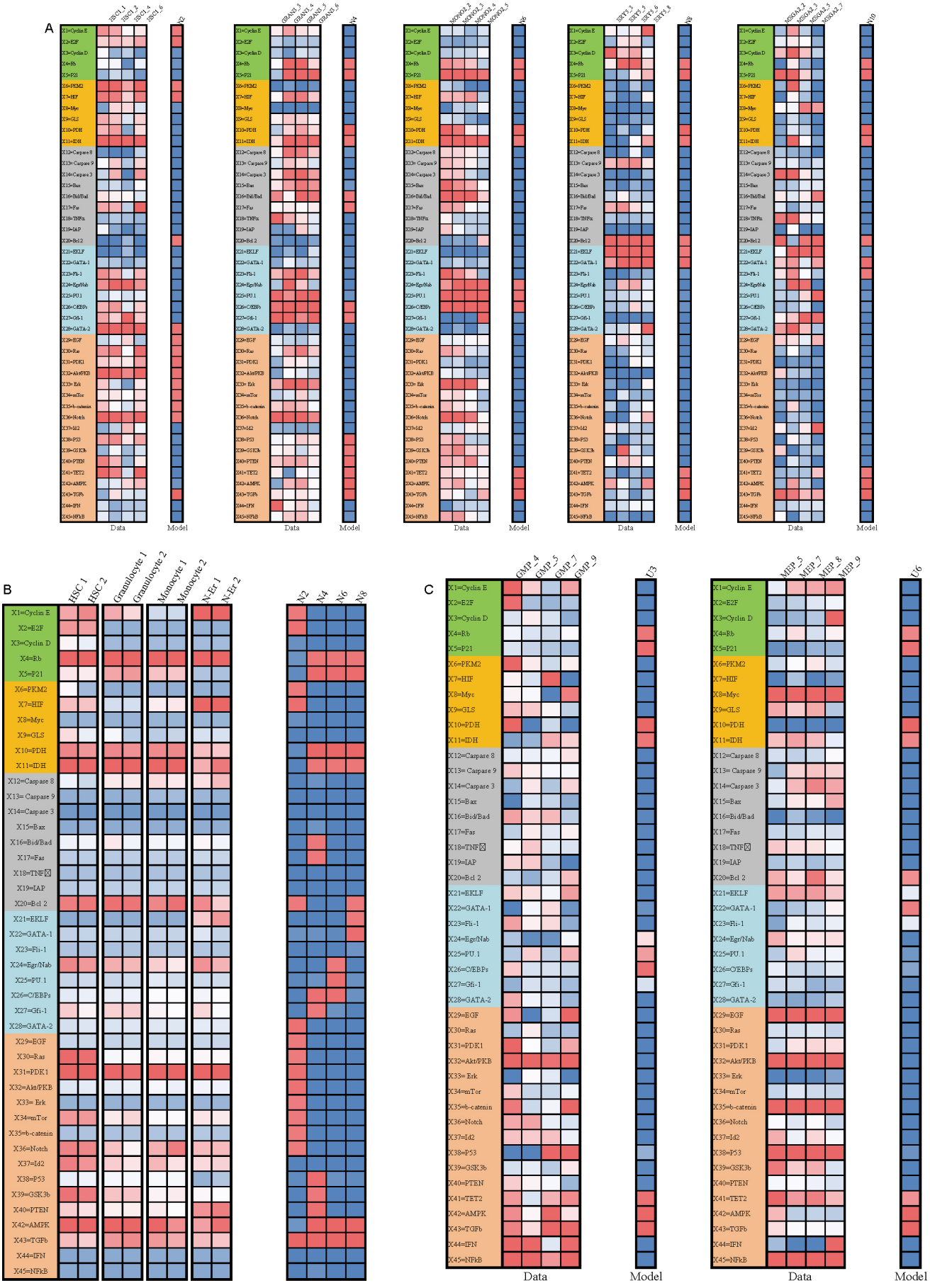
A
B
C
Data
Model

Figure 3 The biological meanings of robust states generated from the core endogenous network were validated at the molecular level. A, We selected the expression data of HSCs, neutrophils, monocytes, erythrocyte and megakaryocytes, in a published dataset collected from human tissue and set a threshold to find out the high or low expressed status of each gene (Novershtern et al., 2011). On the other hand, agent values of stable states N2, N4, N6, N8, and N10 in the model results, which represent the functional status of the five cell types were approximated to activated/inactivated status (represented by 1/0, discussed above). The mean agreements between the model results and experimental data of HSCs, neutrophils, monocytes, erythrocytes, and megakaryocytes are 63%, 60%, 64%, 72%, and 60%, respectively. B, We selected the relevant expression data in a published dataset collected from mice (Chambers et al., 2007) and set a threshold to find out the high or low expressed status of each gene. On the other hand, agent values of stable states N2, N4, N6, and N8, which represent the functional status of the five cell types, HSCs, neutrophils, monocytes, and erythrocytes, are shown in the left. The mean agreements between the model results and experimental data of HSCs, neutrophils, monocytes, erythrocytes, and megakaryocytes are 61%, 69%, 72%, and 62%, respectively. C, In order to validate the biological meanings of unstable states U3 and U6, we selected the expression data of GMPs and MEPs collected from human tissue, and set a threshold to find out the high or low expressed status of each gene (Novershtern et al., 2011). Agent values of unstable states U3 and U6, which represent the functional status of the GMPs and MEPs, respectively, are shown in this heat-map. Compared with this experimental data, the mean agreements between the agent values of unstable states U3 and U6 in the model results and expression data of GMPs and MEPs were 71% and 75%, respectively. Red color denotes the activated/highly-expressed agents, while blue color denotes the inactivated/low-expressed agents.

work described different cell-fates in myeloid development.

Transition states reproduced the core features of cell intermediates

Since the correspondences between robust stable states and distinct cell-fates have been built, further questions naturally arouse: how to interpret the existence of the cell intermediates in the myeloid development? These cell intermediates are quite different from stable cell types in the following three biological aspects (Kondo et al., 2003). Firstly, stem cells will experience a series of intermediate stage before finally developing into specialized cell types. Secondly, cell intermediates are sensitive to extrinsic or intrinsic fluctuations. Upon fluctuations, these cell intermediates can develop into certain cell types. Thirdly, cell intermediates are characterized by their differentiation potential towards specific set of cell types. Mathematically, dynamical system implies the existence of their theoretical counter-parts, called unstable states (Arnold and Levi, 1988). Firstly, it is more probable to pass through certain unstable state when a system transiting from one stable state to another. Secondly, compared with stable states, unstable states are more sensitive to small perturbations. Upon specific perturbations, the system would leave the initial state and evolve to certain stable states. Thirdly, an unstable state connects a specific set of stable states. These similar properties between cell intermediates and unstable states suggested that these structurally robust unstable states of the core endogenous network may have biological meanings as cell intermediates.

Biologically, the functional status of GMPs and MEPs, which occurred in myeloid development, was summarized according to the accumulated experimental observations. GMPs and MEPs were generally characterized by the low self-renewal ability, resistance of cell death and aerobic metabolism to supply energy (Kohli and Passegué, 2014; Kondo et al., 2003). The specifically expressed TFs in GMPs and MEPs were summarized as their differentiation module status (Figure S1 in Supporting Information) (Laslo et al., 2006; Starck et al., 2003). In this context, the functional status of GMPs and MEPs were described as cell cycle "off", apoptosis "off", aerobic metabolism and the co-expressed TFs as their molecular identities (Table 3).

Mathematically, 42 robust unstable states were obtained in the ODE dynamical system (Tables S17−S20 in Supporting Information). Similarly, the biological meanings of the 42 unstable states were discussed at the modular level (Supplementary 4 in Supporting Information). As the lineage-specific TFs served as the molecular identities of specific cell types, these 42 roust unstable states were divided into 10 subclasses (C1−C10) based on their differentiation module status (Tables S22−S30 in Supporting Information). We found that two unstable states, U1 in C1 and U6 in C2, have perfect matches with GMP and MEP respectively at the modular level (Table 3). Furthermore, we validated this conclusion at molecular level, by comparing the agent values of U1 and U6 with the expression data of GMPs and MEPs in a human expression profiling dataset (Novershtern et al., 2011). The agreements between model results and the experimental data were more than 70% (Figure 3C), which suggested that unstable states U1 and U6 corresponded to GMPs and MEPs at the molecular level. Besides the two robust unstable states discussed above, yet another 40 robust unstable states were found in the model (Tables S22−S30, Supplementary 4.2 in Supporting Information).

Briefly, the robust unstable states U1 and U6 of the core endogenous network corresponded to GMP and MEP respectively at both modular and molecular level. These two cases validated the assumption that the structurally robust unstable states of the endogenous network described the cell intermediates in early myeloid development.

Interconnection among robust states indicated the developmental routes

We have shown that the robust stable states of the endogenous network represent the specific myeloid cell-fates and the unstable states represent the cell intermediates. Mathematically, an unstable state connects a specific set of stable states. It is interesting to find out whether the interconnections among these states also have some biological meanings.

We designed an algorithm to get the trajectories from each unstable state to its connected stable states (Models and methods). As discussed above, we found two unstable states U1

Table 3 Validation of unstable states U1 and U6[a)]

	Experimental knowledge		Model results	
Cell type/unstable state	GMP	MEP	U1	U6
Cell cycle	Off	Off	Off	Off
Apoptosis	Off	Off	Off	Off
Metabolism	Aerobic	Aerobic	Aerobic	Aerobic
Differentiation	C/EBPα PU.1 Egr/Nab (antagonist with Gfi-1) Gfi-1 (antagonist with Egr/Nab)	GATA1 EKLF(antagonist with Fli-1) Fli-1(antagonist with EKLF)	PU.1 C/EBPs Egr/Nab^{int} Gfi-1^{int}	GATA-1 EKLF^{int} Fli-1^{int}
Differentiation potential/ Stable states connected	Granulocyte(neutrophils) Monocytes	Erythrocytes Megakaryocyte	N4 (Neutrophils) N6 (Monocytes)	N8 (Erythrocytes) N10 (Megakaryocyte)

a) The functional status and differentiation potential of GMPs and MEPs were summarized from well-documented observations in experiment (Kohli and Passegué, 2014; Kondo et al., 2003; Starck et al., 2003). On the other hand, the module status of unstable states U1, U6 and the stable states connected by them were obtained from the model results. The comparison between model results and experiment observations shows that unstable states U1 and U6 have perfect correspondence with GMPs and MEPs in terms of both module status and differentiation potential. The subscribed "int" denoted the agent with intermediate values.

and U6 corresponded to GMP and MEP at both modular and molecular level. According to the perturbation simulation results, we found that U1 connected the stable state N4 and N6 representing neutrophils and monocytes, while U6 connected the stable state N8 and N10 representing erythrocytes and megakaryocyte respectively. The results perfectly agreed with the known experimental facts about the differentiation potential of GMPs and MEPs (Akashi et al., 2000). In other words, the results suggested that the interconnections among these robust states revealed the developmental routes, which enabled the organization of certain cell-fates into a quantitative dynamical framework to understand the myeloid development.

The landscape as a quantitative scheme to understand early myeloid development

According to the model results, a specific landscape model was obtained as a quantitative scheme to understand the early myeloid development, where structurally robust states correspond to cell phenotypes and their interconnections reveal developmental routes (Figure 4). It not only explained the known experimental observations coherently, but also provided a series of new predictions, which are testable by further experiments.

First of all, the landscape reproduces the standard roadmap model straightforwardly. The stepwise fate-restriction is illustrated as the process that a system (or a cell) overcomes the barrier and gets to a hyper-transition state from certain stem-like states, then rolls down and successively passes through certain unstable states of lower ranks before finally reaching to the specialized cell states (Figure 5A and B). The perturbation results suggest that the hyper-transition states tend to connect more stable states than the transition states (Tables S58−S63 in Supporting Information). Therefore, the gradual cell-fate restriction can be illustrated by reduce of stable states connected by the unstable states along the route. In addition, the molecular dynamics along the developmental route can be predicted from the model results. The endogenous network reproduced the successive dynamical events in the standard model, including the loss of self-renewal capacity, the multi-lineage priming events, and the gradual lineage specification, which perfectly agreed with known facts (Figure 5C).

Secondly, the varying observations of developmental routes are expected, as the landscape suggests multiple trajectories to adopt when transiting from one stable state to another (Figure S2A). The myeloid bypass model (Yamamoto et al., 2013) are explained straightforwardly in the present landscape (Figure 6A and B). The megakaryocytic-biased model (Sanjuan-Pla et al., 2013; Shin et al., 2014), which served as the counterpart of LMPP model (Adolfsson et al., 2005), has also been reproduced in the present quantitative scheme (Figure 6C and D). We further predicted more than one route to achieve the megakaryocytic-biased development (Table S31 in Supporting Information). On the other hand, as the transition between stable states is inter-converted, the observations of cell-fate inter-conversions can be explained straightforwardly in the landscape (Figure S2B in Supporting Information). In specific, we explained the myeloid trans-differentiation under specific gene manipulation from the state transition dynamics of the endogenous network (Table 4). We further predicted the molecular dynamics along these trans-differentiation events in experiment (Figure 7). In principle, varying observations of hematopoietic development can be integrated into a single landscape.

More importantly, the quantitative model shows prediction capacity for cell states and developmental routes, which may have not been noted in experiment before. We found 55 structurally robust states in total, including 13 stable states and 42 unstable states, which were determined by network topology. Here, we will discuss two specific predictions based on the

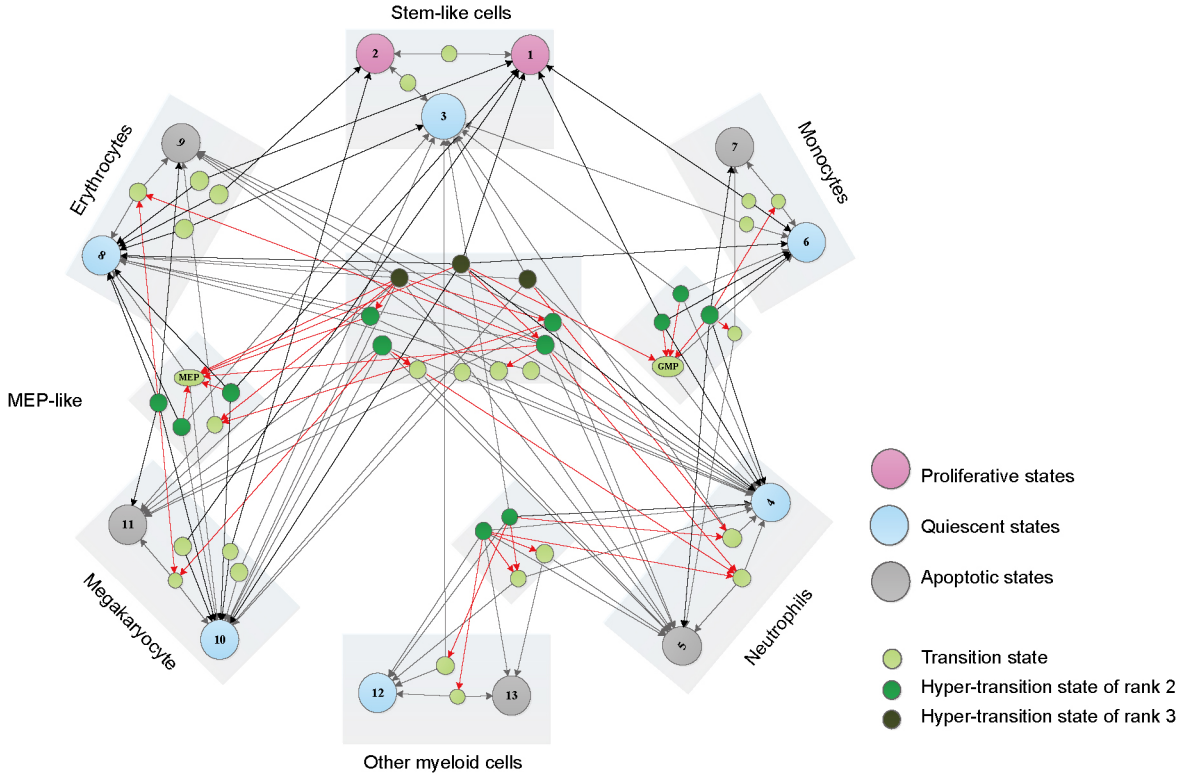

Figure 4 The quantitative developmental scheme generated from the emerging properties of the core endogenous network. These properties illustrated above were computed from the core endogenous network dynamics. The big circles represent the robust stable states, which described different myeloid cell-fates. Among them, pink circles represent the proliferative states with cell cycle "on", apoptosis "off". Blue circles represent the quiescent states with cell cycle "off", apoptosis "off". Grey circles represent the apoptotic states with apoptosis "on". Forty-two robust unstable states are denoted by small green circles: light-green circles represent the transition states (of rank 1); medium-green circles represent the hyper-transition states of rank 2; dark-green circles represent the hyper-transition states of rank 3. According to their differentiation module status, these states were classified into different classes, which were gathered into grey shadows. The relative location among states is denoted by arrows: the interconnections from each unstable state to its connected stable states are denoted by black arrows; trajectories that started from a hyper-transition state and successfully pass through other unstable states of lower ranks are denoted by red arrows. Upon specific induction or noise, the system can transit from one stable state to another, by successively passing through a set of unstable states.

Table 4 The simulation of cell-fate transition[a)]

Original cell types	Manipulation	Resulting cell type	Reference	Molecular dynamics
Erythroid	Inducible PU.1 *expr.	Monocyte	(Yamada et al., 1998)	Figure 6A
MEP	Inducible PU.1 *expr.	Myloid cells	(Nerlov and Graf, 1998)	Figure 6B
GMP	Constant GATA1 *expr.	MEP	(Kulessa et al., 1995)	Figure 6C
Eosinophil	Constant GATA1 *expr.	MEP	(Nerlov et al., 2000)	Figure 6D

a) *expr., expression.

robust transition states (of rank 1) in the quantitative model.

Prediction 1: Non-sequential transitions

We found that a set of transition states (U14, U16, U17, U19, U20, U21, U23, U24, U25) directly connected two stable states representing stem cells and the specialized cell types (Figure 8A, Table S31 in Supporting Information). The differentiation module status of these transition states corresponded to the molecular identities of the relevant specialized cell types. For example, transition state U19 connected the stable state N3 and N8, which represented the quiescent stem cells and the erythrocytes respectively. The differentiation module status of U19 corresponded to the molecular identity of erythrocytes (Laslo et al., 2006; Starck et al., 2003). Accordingly, we predicted the existence of a series of cell intermediates, which not only possess the stem-cell-like potential, but also have strong lineage-bias towards specialized cell types. The developmental routes, tentatively named as non-sequential transitions, were therefore predicted, through which the stem cells may skip some common intermediate states and directly committed into certain cell fates (Figure 8B).

Encouragingly, after we obtained the predictions, a series of studies based on single cell analysis were published and

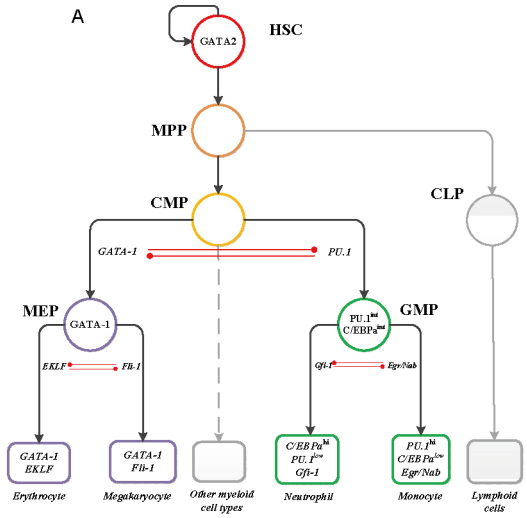
A
HSC
GATA2
MPP
CMP
CLP
GATA-1
PU.1
MEP
GATA-1
GMP
EKLF
Fli-1
Gfi-1
Egr/Nab
GATA-1 EKLF
GATA-1 Fli-1
Erythrocyte
Megakaryocyte
Other myeloid cell types
Neutrophil
Monocyte
Lymphoid cells

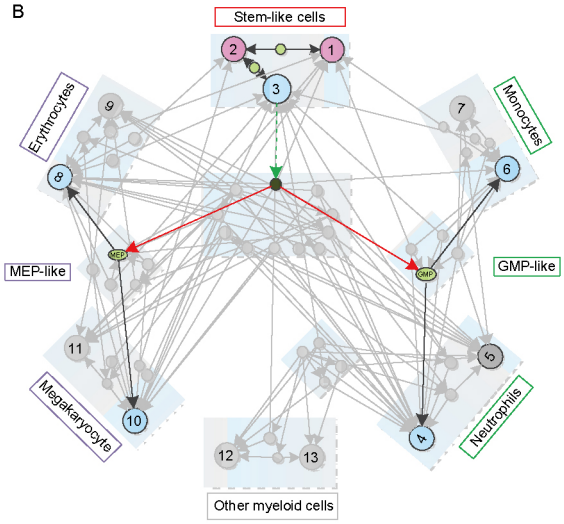
B
Stem-like cells
Erythrocytes
Monocytes
MEP-like
GMP-like
Megakaryocytes
Neutrophils
Other myeloid cells

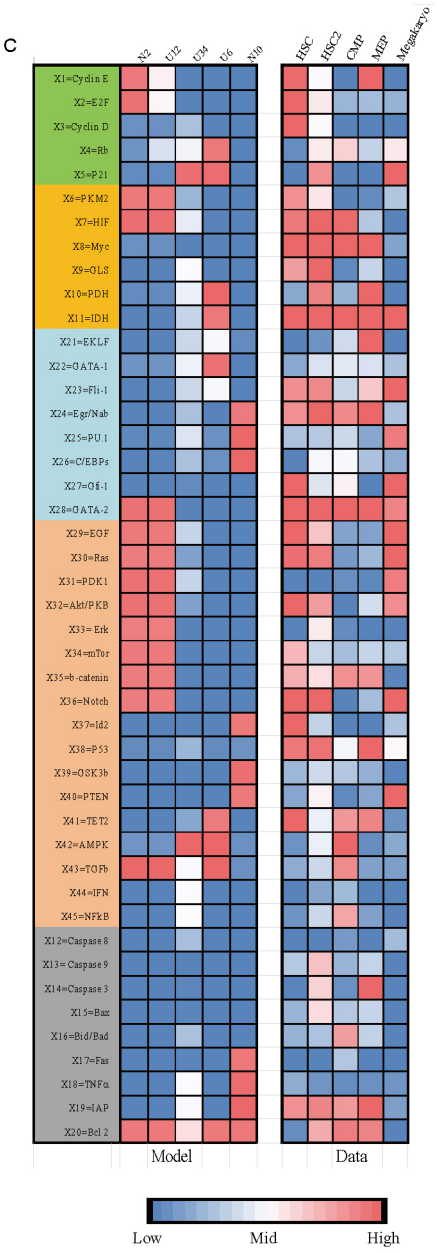
C
N2
U12
U34
U6
N10
HSC
HSC2
CMP
MEP
Megakaryo
X1=Cyclin E
X2=E2F
X3=Cyclin D
X4=Rb
X5=P21
X6=PKM2
X7=HIF
X8=Myc
X9=GLS
X10=PDH
X11=IDH
X21=EKLF
X22=GATA-1
X23=Fli-1
X24=Egr/Nab
X25=PU.1
X26=C/EBPa
X27=Gfi-1
X28=GATA-2
X29=EGF
X30=Ras
X31=PDK1
X32=Akt/PKB
X33=Erk
X34=mTor
X35=b-catenin
X36=Notch
X37=Id2
X38=P53
X39=GSK3b
X40=PTEN
X41=TET2
X42=AMPK
X43=TGFb
X44=IFN
X45=NFkB
X12=Caspase 8
X13=Caspase 9
X14=Caspase 3
X15=Bax
X16=Bid/Bad
X17=Fas
X18=TNFa
X19=IAP
X20=Bcl 2
Model
Data
Low
Mid
High

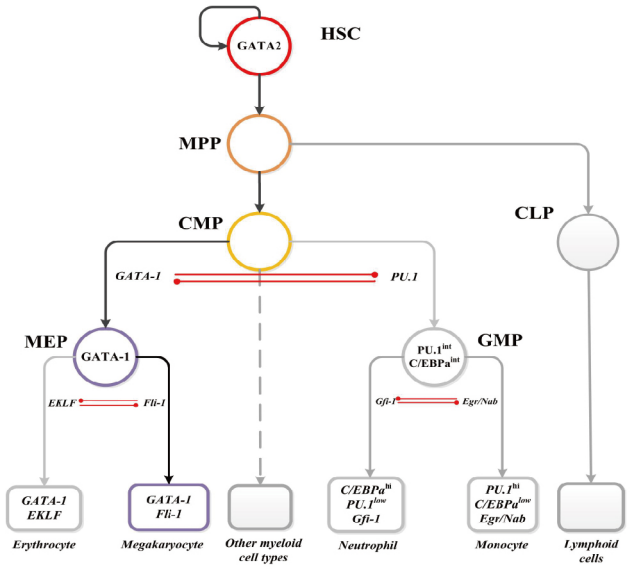
HSC
GATA2
MPP
CMP
CLP
GATA-1
PU.1
MEP
GATA-1
GMP
EKLF
Fli-1
Gfi-1
Egr/Nab
GATA-1 EKLF
GATA-1 Fli-1
Erythrocyte
Megakaryocyte
Other myeloid cell types
Neutrophil
Monocyte
Lymphoid cells

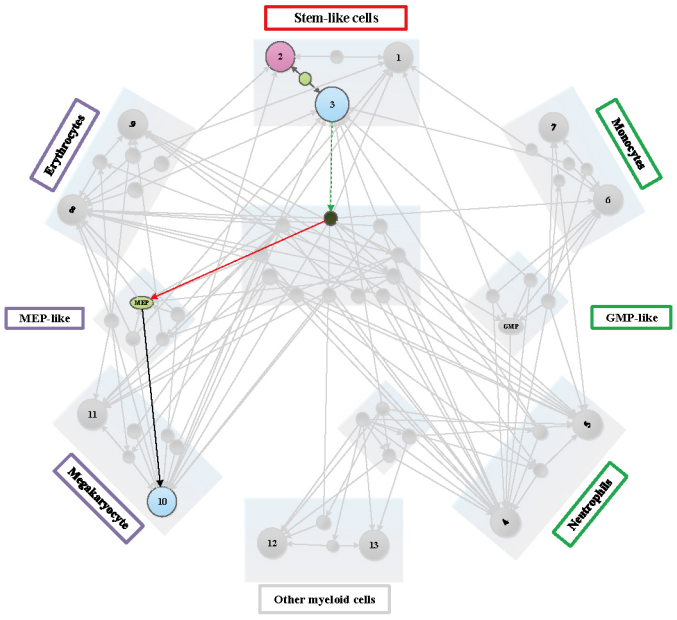
Stem-like cells
Erythrocytes
Monocytes
MEP-like
GMP-like
Megakaryocyte
Neutrophils
Other myeloid cells

Figure 5 The standard roadmap of myeloid development was explained in the present model. A, The standard hematopoietic roadmap has been well established from the experimental observations, which highlight the stepwise and hierarchical manner of hematopoietic development. B, The stepwise fate-restriction in the standard roadmap can be illustrated as the process that a system (or a cell) overcomes the barrier and reaches a hyper-transition state from certain stem-like state, then rolls down and successfully passes through a series of unstable states of lower ranks before finally reaching to the specialized cell state. The differentiation potential of specific cell intermediate is described by the stable states connected by the corresponding unstable state along the route. The system in a stable state can overcome the barrier and transit to certain unstable states, upon specific induction or noise (illustrated by the green dashed line). C, The quantitative model further predicted the molecular dynamics along the standard roadmap: a cell in the proliferating stem-like state (N2) will lose its proliferating ability and reach the quiescent stem-like state (N3). Then the cell will overcome the barrier and reach a hyper-transition state (U34), where multiple lineage-specific TFs will simultaneously express at a low level. This dynamical event has already been observed biologically, namely the multi-lineage priming events (Hu et al., 1997). After that, the cell will go through a gradual cell-fate restriction by passing through a bi-potent state (U6), and finally reach a stable state representing megakaryocyte. The predicted dynamics have a good match with the known knowledge about the standard development. To further validate the prediction, we compare the model results with the expression data (Novershtern et al., 2011), which showed a good agreement (69%).

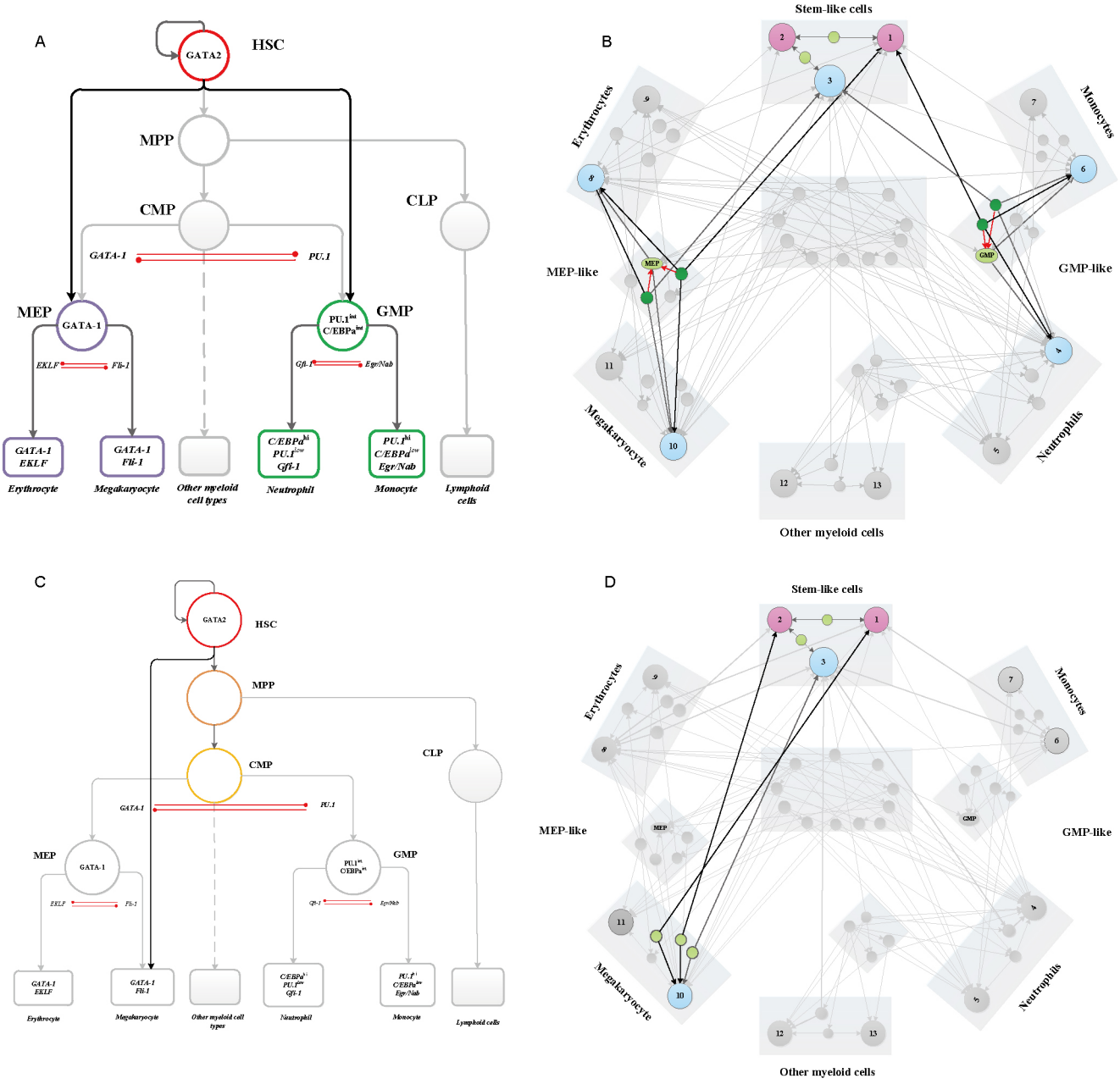

Figure 6 The endogenous network dynamics incorporated the seemingly conflicted roadmap models. The myeloid bypass model (A) in which HSCs directly give rise to myeloid-specific progenitors can be incorporated in the landscape model (B). The megakaryocytic-biased model (C) in which HSCs directly give rise to megakaryocyte-specific progenitors can be incorporated in the landscape model (D). We further predicted three independent routes to achieve megakaryocytic-biased development.

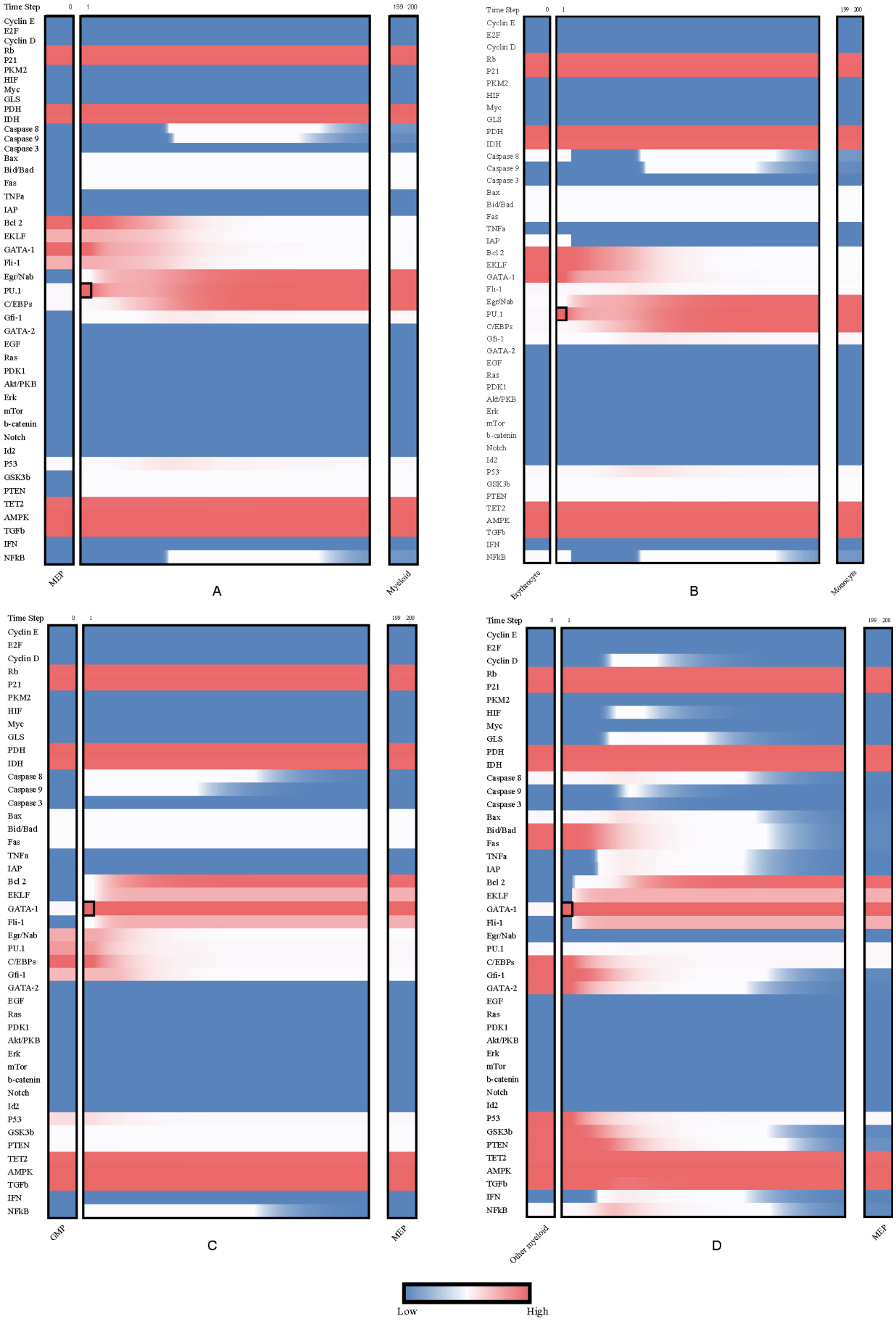
Time Step
0
1
199
200
Cyclin E
E2F
Cyclin D
Rb
P21
PKM2
HIF
Myc
GLS
PDH
IDH
Caspase 8
Caspase 9
Caspase 3
Bax
Bid/Bad
Fas
TNFa
IAP
Bcl 2
EKLF
GATA-1
Fli-1
Egr/Nab
PU.1
C/EBPs
Gfi-1
GATA-2
EGF
Ras
PDK1
Akt/PKB
Erk
mTor
b-catenin
Notch
Id2
P53
GSK3b
PTEN
TET2
AMPK
TGFb
IFN
NFkB
MEP
Myeloid
A
Erythrocyte
Monocyte
B
GMP
MEP
C
Other myeloid
MEP
D
Low
High

Figure 7 The molecular dynamics during the cell-fate transition events. We simulated the cell-fate transition events upon specific gene manipulation. The state transitions in the endogenous network reproduced the cell-fate transition observations (Table 4). We further predicted the molecular dynamics during the cell-fate transition events, which showed strong nonlinear behaviors. The vertical axe indicates the activity or expression level of each agent. The horizontal axe indicates the time steps in the model. Red color denotes the activated/highly-expressed agents, while blue color denotes the inactivated/low-expressed agents.

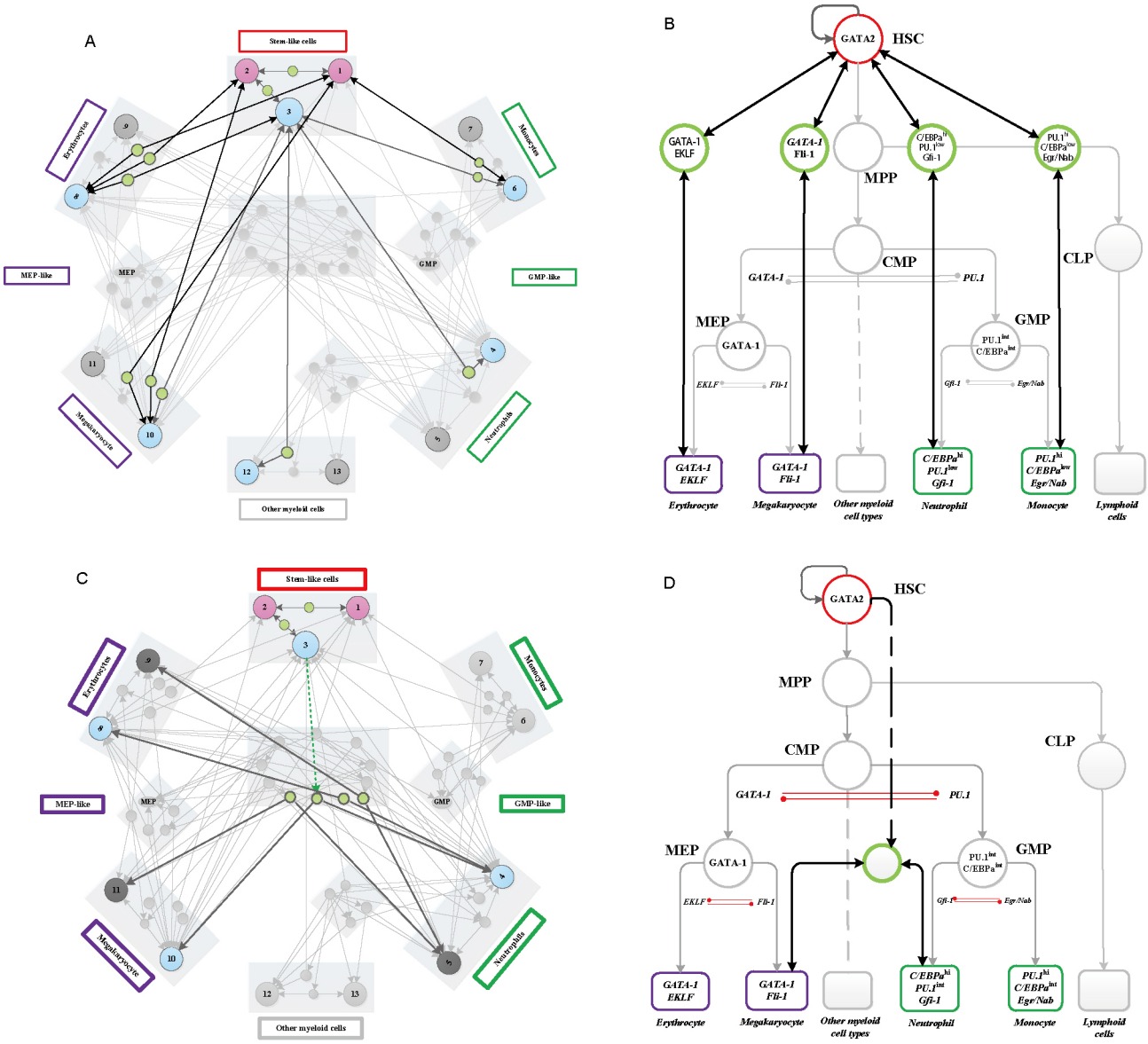

Figure 8 Non-sequential transitions and cross-branch transitions predicted from model. A, Non-sequential transitions: a set of transition states directly connected two stable states representing stem cells and the specialized cell types, whose differentiation module status showed the same status with their connected specialized cell type. The lineage-committed progenitors were predicted accordingly, through which the stem cell could transit directly into these specialized cell types without passing through several common progenitors. B, The non-sequential transitions were predicted to coexist with the stepwise routes. C, Cross-branch transitions: a set of transition states directly connected two stable states representing specialized cell types in distinct branches. The green dashed line illustrates the possible process that a cell in a stable state overcame the barrier and got to the cross-branch transition state upon specific induction. D, The cross-branch routes towards "developmentally distant" cell types were predicted accordingly, which provided additional insights towards the non-hierarchical and flexible feature of myeloid development. The double-side arrow indicates that the transitions between different cell-fates were inter-converted.

revised the stepwise model into a roadmap with cell-fate commitment at early stage (Haas et al., 2015; Notta et al., 2016; Paul et al., 2015; Perié et al., 2015). Among them, the analysis of single cell transcriptional profiling data illustrated the early transcriptional priming towards different cell fates within the early myeloid progenitors, which can be clustered into several subgroups according to their enriched lineage-specific markers and TFs (Paul et al., 2015). We compared the single cell gene expression data (cluster C2, C8, C15, and C9 presenting erythrocyte, megakaryocyte, monocytes and neutrophil markers and TFs in their transcriptome respectively), with the agent values of the predicted

transition states in our model (U21, U24, U17, U14). The single cell transcriptional data and model prediction showed good agreements (Figure 9). The single cell transcriptional data independently validated the model prediction results. Our model results also back up these experimental efforts from mechanistic point of view. We further predicted the inner heterogeneity among these lineage-biased progenitors, which is testable by future experiments.

Prediction 2: Cross-branch transitions

We found another set of transition states (U39, U40, U41, U42), which directly connected two stable states representing specialized cell types in different branches (Figure 8C, Table S32 in Supporting Information). For example, the transition states U42 connected stable states N4 and N8, which represented neutrophil and megakaryocyte respectively. These transition states indicated the existence of the common bi-potent progenitors between these "developmentally distant" cell types. Accordingly, the cross-branch routes towards these cell types were predicted, which highlighted the non-hierarchical and flexible features of hematopoietic development (Figure 8D).

To our knowledge, the predicted cross-branch transitions have not been noted experimentally. Nevertheless, the trans-differentiation between the "long-distant" cell types without passing through the common progenitors was extensively observed upon specific gene manipulation (Graf, 2011; Ladewig et al., 2013). These events served as indirect proofs for the existence of cross-branch transitions. Further experimental efforts are needed to test the predictions by identifying the cell intermediates with differentiation potential towards distinct branches, and the existence of cross-branch developmental routes.

DISCUSSION

The heterogeneity within the classically defined early myeloid progenitors and cell-fate inter-conversion events challenged the roadmap model, which has become difficult to follow up the increasing discoveries with continuous refinement. In this work, we established an integrated quantitative framework of early myeloid development, which not only explained the known experimental observations from the mechanistic point of view, but also provided a series of predictions testable by future experimental efforts. We constructed a core endogenous network of early myeloid cell-fate determination by integrating the molecular interactions independently from accumulated mechanistic knowledge. Structurally robust fixed points of the core endogenous network were obtained, in which agent values were not obvious before analysis in such a high-dimensional and nonlinear dynamical system. Although many details have been simplified in the core endogenous network at the first stage, these robust fixed points have already been able to reproduce the main features of different cell states of the early myeloid development. Further analysis revealed the interconnections among these stable states and unstable states, which enabled a natural organization of certain cell-fates into a landscape. To our knowledge, the present landscape model served as a first quantitative scheme that (i) explained the cell phenotypes and standard scheme of early myeloid development from mechanistic point of view; (ii) is capable of explaining the seemingly conflicting observations, including the varying developmental routes and the cell-fate inter-conversion events; (iii) predicted a complex pool of cell intermediates and developmental routes that can be further tested in experiment. Overall, the quantitative scheme suggested a more complex picture of myeloid development than previous thought and challenged the linear and hierarchical view of development. The quantitative scheme is open to further expansion to explain and predict more features of hematopoiesis and contribute to further regulatory strategies of hematopoiesis.

The present landscape based on a core endogenous network was compared with the other paralleled work as follows.

Endogenous network and gene regulatory networks (GRNs)

The endogenous network was constructed to capture the core molecular mechanism of the early myeloid cell-fate determination process. In the meantime, the bioinformatics obtained Gene Regulatory Networks (GRNs) also have been constructed with similar aims (Klein et al., 2015; Klimmeck et al., 2014; Novershtern et al., 2011). The differences between the core endogenous network and these bioinformatics obtained GRNs were discussed in the following three aspects. Firstly, the endogenous network was constructed by summarizing the well-documented molecular biological and biochemical experiments, whereas the construction of the bioinformatics obtained GRNs was based on statistical analysis of the high through-put data. The reliability of GRNs were limited by both quality and quantity of the available high through-put data (Brenner, 2010). Secondly, the core endogenous network was formed as a causal network, which can be further quantitatively realized as a non-linear dynamical system (Li et al., 2015; Wang et al., 2014a; Wang et al., 2013; Zhu et al., 2015). As contrast, the majority of the data-driven GRNs was currently correlative and networks. Thirdly, the endogenous network incorporated both the gene regulations and signaling transduction in the biological systems. Overall, both of these approaches investigated the genotype-phenotype mapping from distinct directions: the backward approach identifies molecular interaction networks on the basis of correlated molecular behavior, while the forward approach examines the mechanisms through which functional properties arise in the interactions of known components. The com-

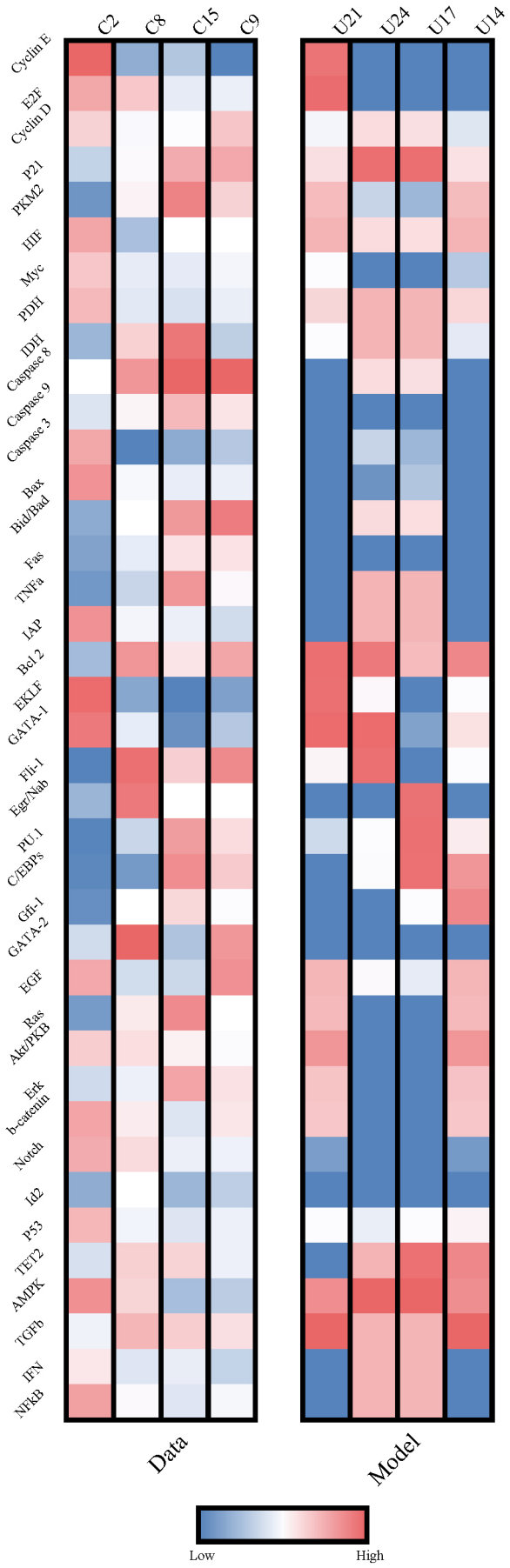

Figure 9 The validation of model prediction 1 from the single cell transcriptional data. Endogenous network suggested that a series of transition states with strong lineage bias in their differentiation module existed in the early myeloid development, which connected stem-like states and specialized cell states directly. Recent single cell transcriptome profiling also illustrated the heterogeneity in early myeloid progenitors, which can be divided into several clusters according to the enriched lineage-defining markers and TFs (Paul et al., 2015). We compared the gene expression of the cluster C2, C8, C15, and C9 with our model prediction (U21, U24, U17, U14), which presented erythrocyte, megakaryocyte, monocytes and neutrophil identities. The agreements between expression data and model predictions are 69.2%, 59.0%, 74.4% and 69.2% respectively. Red color denotes the activated/highly-expressed agents, while blue color denotes the inactivated/low-expressed agents.

mon goal of these two different approaches is "middle-out", to get better understanding of the organization principles underpinning these complex phenomena. The combination of these two approaches has a promising future that will bring biology to the next systematic level.

Other networks which introduced the documented knowledge into the network construction process have also been proposed to study the molecular mechanisms of the hematopoietic systems (Kueh and Rothenberg, 2012; Naldi et al., 2010). Differences between the endogenous network and these networks were discussed as follows. First of all, the universal existence and significance of feedback regulation in the biological system were noted in the construction of endogenous network, which formed an autonomous system. Whereas the organization of many networks based on documented knowledge, such as networks in KEGG, were of input-output type. Secondly, the endogenous network incorporated four functional-independent modules including cell cycle, apoptosis, metabolism and differentiation. The cross-talk regulation between cell proliferation, cell death, metabolism and differentiation provided a holistic understanding towards the molecular mechanisms of the blood homeostasis maintenance.

Comprehensive understanding towards cell-fate determination process

The concept of landscape, which was proposed decades ago (Waddington, 1942; Waddington, 2014), served as a powerful tool to quantitatively and metaphorically describe the complex biological system (Ao, 2009). The genetic and epigenetic effects upon phenotype transitions have been discussed widely (Lei et al., 2014; Li et al., 2016; Wang et al., 2014b). Stable state has been used to represent distinct cell type previously (Ao et al., 2008; Huang et al., 2009). Both cells and cell intermediates were all recognized as stable states and the hematopoietic development has been envisaged as a rough road by passing through a series of basins (Enver et al., 2009).

In the present work we found that the robust stable states of a specific network described certain myeloid cell-fates. We proposed and validated that structurally robust unstable states represented cell intermediates. Two unstable states U1 and

U6 corresponded to GMP and MEP respectively in terms of their module status, gene expression patterns and differentiation potential. The dynamical properties of these unstable states provided insights towards the special characteristics of the cell intermediates, which would help for elucidating the regulation strategies of progenitors. Further, the sensitivity of unstable states also provides possible interpretation of the recent evidences from murine *in situ* tracking experiments, showing that progenitors, rather than the HSCs, are the main drivers of steady-state hematopoiesis during most of adulthood (Busch et al., 2015; Sun et al., 2014). The endogenous network dynamics can guide for directional manipulation of specific cell-fates and contribute to a better understanding of normal blood differentiation programs, which is critical to reveal the diseases genesis in blood system and further benefit the medical advances.

MODELS AND METHODS

Endogenous network construction

The main approach of constructing the core endogenous network of early myeloid cell-fate determination is described as follows. As it is difficult to depict every detail at the first stage due to the complexity of biological systems, we focus on describing the conserved regulatory structure and the core features of early myeloid development, instead of trying to incorporate all of the accumulated regulations. The details are noted in Supplementary Part 1 in Supporting Information.

Firstly, four essential modules, including cell cycle, metabolism, apoptosis and differentiation, were selected to capture the main features of the early myeloid development.

Secondly, each module was simplified by a set of key agents to capture the core functional status according to the accumulated molecular knowledge (Alberts et al., 2008) (Tables S1 and S2 in Supporting Information). In this work, we chose a set of essential proteins to depict their core regulatory structures, since proteins are the main executors of biological function. Taking cell cycle as an example, the two gap phases (G1 and G2 phase) of cell cycle provide time for a cell to monitor the internal and external environment to ensure that conditions are suitable before the cell commits itself to divide (Hartwell and Kastan, 1994; Massagué, 2004). Among them, G1 phase is especially important in this respect. Therefore, the key regulators of the restriction point (R point) in G1 phase, including Cyclin D-CDK4/6 complex, Cyclin E-CDK2, pRb, E2Fs, and p21 were selected to represent the core regulatory mechanisms of cell cycle. In this way, we approximate the cell cycle as bi-stability and mainly focus on describing the 'on' and 'off' status of cell cycle in the coarse-grained quantitative framework. The simplicity of cell cycle has already been applied in the previous quantitative work (Chen et al., 2000; Qu et al., 2003). These selected agents were characterized by their evolutionary conservation.

Thirdly, the construction of endogenous network emphasized the significance of the feed-back loops in biological system, which led to an autonomous system.

Quantitative analysis of the endogenous network

The core endogenous network was quantified and analyzed by using a set of ordinary differential equations (ODEs) and Boolean dynamics respectively.

ODE dynamics

The core endogenous network was firstly described by a set of ODEs (Ao et al., 2010; Glass and Kauffman, 1973). The sigmoid-shaped Hill functions, which have been commonly used to model transcriptional regulations and signaling transductions (Huang and Ferrell, 1996; von Dassow et al., 2000), were adopted in this quantitative framework to describe the activation/inhibition among agents. Two independent algorithms were designed to find the structurally robust states in these dynamical systems. The details are stated in Supplementary Part 2.1 in Supporting Information.

Boolean dynamics

In Boolean network, the expression of each agent was approximated by only two states: active and inactive (represented by 1/0). The values were updated in discrete time step. The state changes of an individual agent were specified by the Boolean rules f, which were transformed from the network structure by using Boolean logic functions: AND, OR, and NOT. The algorithm was designed to calculate the stable states of the Boolean dynamical system. The details are stated in Supplementary Part 2.2 in Supporting Information.

State interconnection analysis

The algorithm was designed to get the trajectories from each unstable state to its relevant stable states. We perturbed the system with small random vectors when it stayed at a certain unstable state. We obtained the trajectories from each unstable state to the connected stable states. We recorded stable states connected by each unstable state and the evolving trajectories (Tables S18−S21 in Supporting Information). The details can be seen in Supplementary 2.3 in Supporting Information.

Significance of multi-stability of endogenous network dynamics

This test assesses the statistical significance of the multi-stable states generated from the core endogenous network versus what would be expected by chance. We defined Q_{stable} as the number of stable states that can be generated in a single network. Our null hypothesis is that the multi-stable states are expected if 177 activated/inhibited interactions among the 45 agents were assigned at random. To test this hypothesis, we

generated more than 10,000 randomized networks, in which the number of agents and interactions is fixed. We quantified the networks by using Boolean analysis and computed the number of stable states Q_{stable} in each randomized network. We compared the resulting distribution with the number of stable states generated by the endogenous network. For the endogenous network, we found the Q_{stable}=13, whereas for all the randomized network we found Q_{stable}=0.9389±1.5162. In a one-tailed test, the P value can be computed as the probability of observing 13 or more stable states generated from a randomized network ($P<10^{-3}$). Assuming the number of stable states comply with normal distribution, we further use student's t test to calculate the P value for the number of stable states ($P_{stable}<10^{-14}$).

Module analysis of the structurally robust states

The status of cell cycle, apoptosis, metabolism and differentiation was specified by the agent values in each module. Accordingly, the biological meanings of each state were discussed. Upon the differentiation module status, the robust states were classified into different groups or subclasses. The details are elaborated in Supplementary Part 3 in Supporting Information.

Comparison with gene profiling data

We validated the model results at the expression level by taking advantage of two independent published datasets collected from humans and mice respectively (Chambers et al., 2007; Novershtern et al., 2011). We set a threshold to find out the "On" or "Off" status of each gene and compared the data with the corresponding states in the model results, where the agent values can be approximated to activated or inactivated (shown as 1/0). The details can be seen in Supplementary Part 5 in Supporting Information. The data sets validating the model results are available on http://ncbi.nlm.nih.gov/geo/, GSE24759, and GSE6506.

Compliance and ethics *The author(s) declare that they have no conflict of interest.*

Acknowledgements *We thank Dr. Qing Nie, Dr. Xiaolong Liu, Dr. Ruibao Ren for insightful comments. We thank our lab members for critical discussions, Haowen Cao for a critical reading of the manuscript, and Tiantian Wu for a drawing artwork. This work was supported by the National Basic Research Program of China (2010CB529200) and National Natural Science Foundation of China (91029738).*

Adolfsson, J., Mansson, R., Buza-Vidas, N., Hultquist, A., Liuba, K., Jensen, C.T., Bryder, D., Yang, L., Borge, O.J., Thoren, L.A.M., Anderson, K., Sitnicka, E., Sasaki, Y., Sigvardsson, M., and Jacobsen, S.E.W. (2005). Identification of Flt3+ lympho-myeloid stem cells lacking erythro-megakaryocytic potential. Cell 121, 295–306.

Akashi, K., Traver, D., Miyamoto, T., and Weissman, I.L. (2000). A clonogenic common myeloid progenitor that gives rise to all myeloid lineages. Nature 404, 193–197.

Alberts, B., Wilson, J.H., and Hunt, T. (2008). Molecular Biology of the Cell, 5th ed. (New York: Garland Science).

Ao, P. (2007). Orders of magnitude change in phenotype rate caused by mutation. Cell Oncol 29, 67–69.

Ao, P. (2009). Global view of bionetwork dynamics: adaptive landscape. J Genets Genomics 36, 63–73.

Ao, P., Galas, D., Hood, L., Yin, L., and Zhu, X.M. (2010). Towards predictive stochastic dynamical modeling of cancer genesis and progression. Interdiscip Sci Comput Life Sci 2, 140–144.

Ao, P., Galas, D., Hood, L., and Zhu, X. (2008). Cancer as robust intrinsic state of endogenous molecular-cellular network shaped by evolution. Med Hypotheses 70, 678–684.

Arnold, V.I., and Levi, M. (1988). Geometrical methods in the theory of ordinary differential equations, 2nd ed. (New York: Springer-Verlag).

Brenner, S. (2010). Sequences and consequences. Philos Trans R Soc B-Biol Sci 365, 207–212.

Bryder, D., Rossi, D.J., and Weissman, I.L. (2006). Hematopoietic stem cells. Am J Pathol 169, 338–346.

Busch, K., Klapproth, K., Barile, M., Flossdorf, M., Holland-Letz, T., Schlenner, S.M., Reth, M., Höfer, T., and Rodewald, H.R. (2015). Fundamental properties of unperturbed haematopoiesis from stem cells *in vivo*. Nature 518, 542–546.

Cahan, P., Li, H., Morris, S.A., Lummertz da Rocha, E., Daley, G.Q., and Collins, J.J. (2014). CellNet: network biology applied to stem cell engineering. Cell 158, 903–915.

Chambers, S.M., Boles, N.C., Lin, K.Y.K., Tierney, M.P., Bowman, T.V., Bradfute, S.B., Chen, A.J., Merchant, A.A., Sirin, O., Weksberg, D.C., Merchant, M.G., Fisk, C.J., Shaw, C.A., and Goodell, M.A. (2007). Hematopoietic fingerprints: an expression database of stem cells and their progeny. Cell Stem Cell 1, 578–591.

Chen, K.C., Csikasz-Nagy, A., Gyorffy, B., Val, J., Novak, B., and Tyson, J.J. (2000). Kinetic analysis of a molecular model of the budding yeast cell cycle. Mol Biol Cell 11, 369–391.

Coussens, L.M., and Werb, Z. (2002). Inflammation and cancer. Nature 420, 860–867.

Enver, T., Pera, M., Peterson, C., and Andrews, P.W. (2009). Stem cell states, fates, and the rules of attraction. Cell Stem Cell 4, 387–397.

Folmes, C.D.L., Dzeja, P.P., Nelson, T.J., and Terzic, A. (2012). Metabolic plasticity in stem cell homeostasis and differentiation. Cell Stem Cell 11, 596–606.

Glass, L., and Kauffman, S.A. (1973). The logical analysis of continuous, non-linear biochemical control networks. J Theor Biol 39, 103–129.

Graf, T. (2002). Differentiation plasticity of hematopoietic cells. Blood 99, 3089–3101.

Graf, T. (2011). Historical origins of transdifferentiation and reprogramming. Cell Stem Cell 9, 504–516.

Grass, J.A., Jing, H., Kim, S.I., Martowicz, M.L., Pal, S., Blobel, G.A., and Bresnick, E.H. (2006). Distinct functions of dispersed GATA factor complexes at an endogenous gene locus. Mol Cellular Biol 26, 7056–7067.

Haas, S., Hansson, J., Klimmeck, D., Loeffler, D., Velten, L., Uckelmann, H., Wurzer, S., Prendergast, Á.M., Schnell, A., Hexel, K., Santarella-Mellwig, R., Blaszkiewicz, S., Kuck, A., Geiger, H., Milsom, M.D., Steinmetz, L.M., Schroeder, T., Trumpp, A., Krijgsveld, J., and Essers, M.A.G. (2015). Inflammation-induced emergency megakaryopoiesis driven by hematopoietic stem cell-like megakaryocyte progenitors. Cell Stem Cell 17, 422–434.

Hanahan, D., and Weinberg, R.A. (2000). The hallmarks of cancer. Cell 100, 57–70.

Hanahan, D., and Weinberg, R.A. (2011). Hallmarks of cancer: the next generation. Cell 144, 646–674.

Hartwell, L.H., and Kastan, M.B. (1994). Cell cycle control and cancer. Science 266, 1821–1828.

Hu, M., Krause, D., Greaves, M., Sharkis, S., Dexter, M., Heyworth, C., and Enver, T. (1997). Multilineage gene expression precedes commitment in

the hemopoietic system.. Genes Dev 11, 774–785.
Huang, C.Y.F., and Ferrell, J.E. (1996). Ultrasensitivity in the mitogen-activated protein kinase cascade. Proc Natl Acad Sci USA 93, 10078–10083.
Huang, S., Ernberg, I., and Kauffman, S. (2009). Cancer attractors: A systems view of tumors from a gene network dynamics and developmental perspective. Seminars Cell Dev Biol 20, 869–876.
Iwasaki, H., Mizuno, S., Arinobu, Y., Ozawa, H., Mori, Y., Shigematsu, H., Takatsu, K., Tenen, D.G., and Akashi, K. (2006). The order of expression of transcription factors directs hierarchical specification of hematopoietic lineages. Genes Dev 20, 3010–3021.
Ji, S., Zhang, L., and Hui, L. (2013). Cell fate conversion: Direct induction of hepatocyte-like cells from fibroblasts. J Cell Biochem 114, 256–265.
Klein, A.M., Mazutis, L., Akartuna, I., Tallapragada, N., Veres, A., Li, V., Peshkin, L., Weitz, D.A., and Kirschner, M.W. (2015). Droplet barcoding for single-cell transcriptomics applied to embryonic stem cells. Cell 161, 1187–1201.
Klimmeck, D., Cabezas-Wallscheid, N., Reyes, A., von Paleske, L., Renders, S., Hansson, J., Krijgsveld, J., Huber, W., and Trumpp, A. (2014). Transcriptome-wide profiling and posttranscriptional analysis of hematopoietic stem/progenitor cell differentiation toward myeloid commitment. Stem Cell Rep 3, 858–875.
Kohli, L., and Passegué, E. (2014). Surviving change: the metabolic journey of hematopoietic stem cells. Trends Cell Biol 24, 479–487.
Kondo, M., Wagers, A.J., Manz, M.G., Prohaska, S.S., Scherer, D.C., Beilhack, G.F., Shizuru, J.A., and Weissman, I.L. (2003). Biology of hematopoietic stem cells and progenitors: Implications for Clinical Application. Annu Rev Immunol 21, 759–806.
Kondo, M., Weissman, I.L., and Akashi, K. (1997). Identification of clonogenic common lymphoid progenitors in mouse bone marrow. Cell 91, 661–672.
Kueh, H.Y., and Rothenberg, E.V. (2012). Regulatory gene network circuits underlying T cell development from multipotent progenitors. WIREs Syst Biol Med 4, 79–102.
Kulessa, H., Frampton, J., and Graf, T. (1995). GATA-1 reprograms avian myelomonocytic cell lines into eosinophils, thromboblasts, and erythroblasts. Genes Dev 9, 1250–1262.
Ladewig, J., Koch, P., and Brustle, O. (2013). Leveling Waddington: the emergence of direct programming and the loss of cell fate hierarchies. Nat Rev Mol Cell Biol 14, 225–236.
Laiosa, C.V., Stadtfeld, M., and Graf, T. (2006). Determinants of lymphoid-myeloid lineage diversification. Annu Rev Immunol 24, 705–738.
Laslo, P., Spooner, C.J., Warmflash, A., Lancki, D.W., Lee, H.J., Sciammas, R., Gantner, B.N., Dinner, A.R., and Singh, H. (2006). Multilineage transcriptional priming and determination of alternate hematopoietic cell fates. Cell 126, 755–766.
Lei, J., Levin, S.A., and Nie, Q. (2014). Mathematical model of adult stem cell regeneration with cross-talk between genetic and epigenetic regulation. Proc Natl Acad Sci USA 111, E880–E887.
Li, C., Hong, T., and Nie, Q. (2016). Quantifying the landscape and kinetic paths for epithelial–mesenchymal transition from a core circuit. Phys Chem Chem Phys 18, 17949–17956.
Li, S., Zhu, X., Liu, B., Wang, G., and Ao, P. (2015). Endogenous molecular network reveals two mechanisms of heterogeneity within gastric cancer. Oncotarget 6, 13607–13627.
Massagué, J. (2004). G1 cell-cycle control and cancer. Nature 432, 298–306.
Naldi, A., Carneiro, J., Chaouiya, C., and Thieffry, D. (2010). Diversity and plasticity of Th cell types predicted from regulatory network modelling. PLoS Comput Biol 6, e1000912.
Nerlov, C., and Graf, T. (1998). PU. 1 induces myeloid lineage commitment in multipotent hematopoietic progenitors. Genes Dev 12, 2403–2412.
Nerlov, C., Querfurth, E., Kulessa, H., and Graf, T. (2000). GATA-1 interacts with the myeloid PU. 1 transcription factor and represses PU. 1-dependent transcription. Blood 95, 2543–2551.
Notta, F., Zandi, S., Takayama, N., Dobson, S., Gan, O.I., Wilson, G., Kaufmann, K.B., McLeod, J., Laurenti, E., Dunant, C.F., McPherson, J.D., Stein, L.D., Dror, Y., and Dick, J.E. (2016). Distinct routes of lineage development reshape the human blood hierarchy across ontogeny. Science 351, aab2116–aab2116.
Novershtern, N., Subramanian, A., Lawton, L.N., Mak, R.H., Haining, W.N., McConkey, M.E., Habib, N., Yosef, N., Chang, C.Y., Shay, T., Frampton, G.M., Drake, A.C.B., Leskov, I., Nilsson, B., Preffer, F., Dombkowski, D., Evans, J.W., Liefeld, T., Smutko, J.S., Chen, J., Friedman, N., Young, R.A., Golub, T.R., Regev, A., and Ebert, B.L. (2011). Densely interconnected transcriptional circuits control cell states in human hematopoiesis. Cell 144, 296–309.
Orkin, S.H., and Zon, L.I. (2008). Hematopoiesis: an evolving paradigm for stem cell biology. Cell 132, 631–644.
Paul, F., Arkin, Y., Giladi, A., Jaitin, D.A., Kenigsberg, E., Keren-Shaul, H., Winter, D., Lara-Astiaso, D., Gury, M., Weiner, A., David, E., Cohen, N., Lauridsen, F.K.B., Haas, S., Schlitzer, A., Mildner, A., Ginhoux, F., Jung, S., Trumpp, A., Porse, B.T., Tanay, A., and Amit, I. (2015). Transcriptional heterogeneity and lineage commitment in myeloid progenitors. Cell 163, 1663–1677.
Perié, L., Duffy, K.R., Kok, L., de Boer, R.J., and Schumacher, T.N. (2015). The branching point in erythro-myeloid differentiation. Cell 163, 1655–1662.
Qian, H. (2013). Stochastic physics, complex systems and biology. Quant Biol 1, 50–53.
Qu, Z., Weiss, J.N., and MacLellan, W.R. (2003). Regulation of the mammalian cell cycle: a model of the G1-to-S transition. AJP-Cell Physiol 284, C349–C364.
Riddell, J., Gazit, R., Garrison, B.S., Guo, G., Saadatpour, A., Mandal, P.K., Ebina, W., Volchkov, P., Yuan, G.C., Orkin, S.H., and Rossi, D.J. (2014). Reprogramming committed murine blood cells to induced hematopoietic stem cells with defined factors. Cell 157, 549–564.
Rosenbauer, F., and Tenen, D.G. (2007). Transcription factors in myeloid development: balancing differentiation with transformation. Nat Rev Immunol 7, 105–117.
Sanjuan-Pla, A., Macaulay, I.C., Jensen, C.T., Woll, P.S., Luis, T.C., Mead, A., Moore, S., Carella, C., Matsuoka, S., Bouriez Jones, T., Chowdhury, O., Stenson, L., Lutteropp, M., Green, J.C.A., Facchini, R., Boukarabila, H., Grover, A., Gambardella, A., Thongjuea, S., Carrelha, J., Tarrant, P., Atkinson, D., Clark, S.A., Nerlov, C., and Jacobsen, S.E.W. (2013). Platelet-biased stem cells reside at the apex of the haematopoietic stem-cell hierarchy. Nature 502, 232–236.
Shin, J.Y., Hu, W., Naramura, M., and Park, C.Y. (2014). High c-Kit expression identifies hematopoietic stem cells with impaired self-renewal and megakaryocytic bias. J Exp Med 211, 217–231.
Starck, J., Cohet, N., Gonnet, C., Sarrazin, S., Doubeikovskaia, Z., Doubeikovski, A., Verger, A., Duterque-Coquillaud, M., and Morle, F. (2003). Functional cross-antagonism between transcription factors FLI-1 and EKLF. Mol Cellular Biol 23, 1390–1402.
Sun, J., Ramos, A., Chapman, B., Johnnidis, J.B., Le, L., Ho, Y.J., Klein, A., Hofmann, O., and Camargo, F.D. (2014). Clonal dynamics of native haematopoiesis. Nature 514, 322–327.
Takahashi, K., and Yamanaka, S. (2015). A developmental framework for induced pluripotency. Development 142, 3274–3285.
Tang, Y., Yuan, R., and Ao, P. (2014a). Nonequilibrium work relation beyond the Boltzmann-Gibbs distribution. Phys Rev E 89, 062112.
Tang, Y., Yuan, R., and Ao, P. (2014b). Summing over trajectories of stochastic dynamics with multiplicative noise. J Chem Phys 141, 044125.
Tang, Y., Yuan, R., Chen, J., and Ao, P. (2014c). Controlling symmetry-breaking states by a hidden quantity in multiplicative noise. Phys Rev E 90, 052121.
Tenen, D.G. (2003). Disruption of differentiation in human cancer: AML shows the way. Nat Rev Cancer 3, 89–101.
Thomas, R., Thieffry, D., and Kaufman, M. (1995). Dynamical behaviour of biological regulatory networks—I. Biological role of feedback loops and practical use of the concept of the loop-characteristic state. Bull Math Biol 57, 247–276.

von Dassow, G., Meir, E., Munro, E.M., and Odell, G.M. (2000). The segment polarity network is a robust developmental module. Nature 406, 188–192.
Waddington, C.H. (1942). Canalization of development and the inheritance of acquired characters. Nature 150, 563–565.
Waddington, C.H. (2014). The strategy of the genes. (New York & London: Routledge).
Wang, G., Su, H., Yu, H., Yuan, R., Zhu, X., and Ao, P. (2016). Endogenous network states predict gain or loss of functions for genetic mutations in hepatocellular carcinoma. J R Soc Interface 13, 20151115.
Wang, G., Zhu, X., Gu, J., and Ao, P. (2014a). Quantitative implementation of the endogenous molecular-cellular network hypothesis in hepatocellular carcinoma. Interface Focus 4, 20130064–20130064.
Wang, G., Zhu, X., Hood, L., and Ao, P. (2013). From Phage lambda to human cancer: endogenous molecular-cellular network hypothesis. Quant Biol 1, 32–49.
Wang, P., Song, C., Zhang, H., Wu, Z., Tian, X.J., and Xing, J. (2014b). Epigenetic state network approach for describing cell phenotypic transitions. Interface Focus 4, 20130068–20130068.
Weissman, I.L. (2000). Stem cells. Cell 100, 157–168.
Wright, S. (1932). The roles of mutation, inbreeding, crossbreeding, and selection in evolution. Proc Sixth Int Congr Genet 1, 356–366.
Yamada, T., Kihara-Negishi, F., Yamamoto, H., Yamamoto, M., Hashimoto, Y., and Oikawa, T. (1998). Reduction of DNA binding activity of the GATA-1 transcription factor in the apoptotic process induced by overexpression of PU. 1 in murine erythroleukemia cells. Exp Cell Res 245, 186–194.
Yamamoto, R., Morita, Y., Ooehara, J., Hamanaka, S., Onodera, M., Rudolph, K.L., Ema, H., and Nakauchi, H. (2013). Clonal analysis unveils self-renewing lineage-restricted progenitors generated directly from hematopoietic stem cells. Cell 154, 1112–1126.
Young, N.S., Scheinberg, P., and Calado, R.T. (2008). Aplastic anemia. Curr Opin Hematology 15, 162–168.
Yuan, R., and Ao, P. (2012). Beyond ito versus stratonovich. J Stat Mech: Theory and Exp 2012, P07010.
Yuan, R., Zhu, X., Radich, J.P., and Ao, P. (2016). From molecular interaction to acute promyelocytic leukemia: Calculating leukemogenesis and remission from endogenous molecular-cellular network. Sci Rep 6, 24307.
Yuan, R., Zhu, X., Wang, G., Li, S., and Ao, P. (2017). Cancer as robust intrinsic state shaped by evolution: a key issues review. Rep Prog Phys 80, 042701.
Zhao, M., and Li, L. (2015). Regulation of hematopoietic stem cells in the niche. Sci China Life Sci 58, 1209–1215.
Zhu, X., Yuan, R., Hood, L., and Ao, P. (2015). Endogenous molecular-cellular hierarchical modeling of prostate carcinogenesis uncovers robust structure. Prog Biophys Mol Biol 117, 30–42.
Zhu, X.M., Yin, L., Hood, L., and Ao, P. (2004). Robustness, stability and efficiency of phage λ genetic switch: dynamical structure analysis. J Bioinform Comput Biol 02, 785–817.

SUPPORTING INFORMATION

1. The construction of the core endogenous network of early myeloid cell-fate determination process
2. Quantitative analysis of the endogenous network
3. Module analysis of the robust stable states and their biological meanings
4. Module analysis of the robust unstable states and their biological meanings
5. Validation of the biological meanings of the robust fixed points at molecular level
6. Supplementary Figures
7. Supplementary Tables

The supporting information is available online at life.scichina.com and link.springer.com. The supporting materials are published as submitted, without typesetting or editing. The responsibility for scientific accuracy and content remains entirely with the authors.